

# Development of a novel, quantitative protein microarray platform for the multiplexed serological analysis of autoantibodies to cancer-testis antigens

Natasha Beeton-Kempen<sup>1,2\*</sup>, Jessica Duarte<sup>1\*</sup>, Aubrey Shoko<sup>3</sup>, Jean-Michel Serufuri<sup>1</sup>, Thomas John<sup>4,5</sup>, Jonathan Cebon<sup>4,5</sup> and Jonathan Blackburn<sup>1</sup>

<sup>1</sup>Institute of Infectious Disease and Molecular Medicine/Division of Medical Biochemistry, University of Cape Town, Cape Town, South Africa

<sup>2</sup>Biosciences Division, Council for Scientific and Industrial Research, Pretoria, South Africa

<sup>3</sup>Centre for Proteomic and Genomic Research, Cape Town, South Africa

<sup>4</sup>Ludwig Institute for Cancer Research, Melbourne, Australia

<sup>5</sup>Joint Ludwig-Austin Oncology Unit, Austin Health, Victoria, Australia

The cancer-testis antigens are a group of unrelated proteins aberrantly expressed in various cancers in adult somatic tissues. This aberrant expression can trigger spontaneous immune responses, a phenomenon exploited for the development of disease markers and therapeutic vaccines. However, expression levels often vary amongst patients presenting the same cancer type, and these antigens are therefore unlikely to be individually viable as diagnostic or prognostic markers. Nevertheless, patterns of antigen expression may provide correlates of specific cancer types and disease progression. Herein, we describe the development of a novel, readily customizable cancer-testis antigen microarray platform together with robust bioinformatics tools, with which to quantify anti-cancer testis antigen autoantibody profiles in patient sera. By exploiting the high affinity between autoantibodies and tumor antigens, we achieved linearity of response and an autoantibody quantitation limit in the pg/mL range—equating to a million-fold serum dilution. By using oriented attachment of folded, recombinant antigens and a polyethylene glycol microarray surface coating, we attained minimal non-specific antibody binding. Unlike other proteomics methods, which typically use lower affinity interactions between monoclonal antibodies and tumor antigens for detection, the high sensitivity and specificity realized using our autoantibody-based approach may facilitate the development of better cancer biomarkers, as well as potentially enabling pre-symptomatic diagnosis. We illustrated the usage of our platform by monitoring the response of a melanoma patient cohort to an experimental therapeutic NY-ESO-1-based cancer vaccine; *inter alia*, we found evidence of determinant spreading in individual patients, as well as differential CT antigen expression and epitope usage.

The cancer-testis (CT) antigen family are a group of > 90 structurally and functionally unrelated proteins usually only expressed in the germ cells in the adult testis or ovary and in the trophoblast of the placenta,<sup>1</sup> but which are aberrantly expressed in various cancers in adult somatic tissues as a

result of disrupted gene regulation. As the testis is an immune-privileged site, aberrant expression of these proteins in somatic tissues typically triggers a spontaneous immune response to the relevant CT antigen. CT antigens have therefore been exploited as therapeutic tumor vaccines,

**Key words:** tumor immunology, predictive markers, cancer diagnosis, cancer-testis antigens, antigen microarrays

**Abbreviations:** BCCP: biotin carboxyl carrier protein; BSA: bovine serum albumin; CT100: cancer-testis antigen array; CT antigens: cancer-testis antigens; CV: coefficient of variation; ELISA: enzyme-linked immunosorbent assay; HRP: horseradish peroxidase; IgG: immunoglobulin G; P117: Patient 117; PBS: phosphate-buffered saline solution; PBST: phosphate-buffered saline solution supplemented with 0.1% Tween-20; PEG: polyethylene glycol; PMT: photomultiplier tube; PPB: potassium phosphate buffer; RFU: relative fluorescent units; SD: standard deviation; SDS-PAGE: sodium dodecyl sulfate-polyacrylamide gel electrophoresis; sIgG: sheep IgG

Additional Supporting Information may be found in the online version of this article.

\*N.B.-K. and J.D. contributed equally to this work

**Grant sponsor:** Cancer Research Institute (USA), Ludwig Institute for Cancer Research and CSL; **Grant number:** LUD2002-013; **Grant sponsors:** National Research Foundation (South Africa), Operational Infrastructure Support Program (Victorian State Government, Australia)

**DOI:** 10.1002/ijc.28832

**History:** Received 19 Dec 2013; Accepted 18 Feb 2014; Online 6 Mar 2014

**Correspondence to:** Jonathan Blackburn, South African Research Chair in Applied Proteomics and Chemical Biology, N3.06 Werner Beit North Building, Institute of Infectious Disease and Molecular Medicine Faculty of Health Sciences, University of Cape Town, Anzio Road, Observatory, Cape Town 7925, South Africa, Tel.: +27-21-406-6071, Fax: +27-21-650-4833, E-mail: jonathan.blackburn@uct.ac.za

**What's new?**

The cancer-testis antigens are a group of unrelated proteins aberrantly expressed in various cancers. Patterns of antigen expression may potentially provide correlates of specific cancer types and disease progression. This study presents a novel microarray platform for high-throughput quantitation of anti-cancer-testis antigen autoantibody profiles in patient sera. Exploiting the higher affinity of autoantibodies, and optimized surface engineering to minimize non-specific signal, the authors achieved linearity of response and a pg/ml quantitation limit. They illustrated the utility of the method by monitoring patient response to an experimental cancer vaccine, finding evidence of differential expression and epitope utilization, and of determinant spreading.

as well as potential prognostic markers in a variety of tumor types.<sup>2</sup>

Increasing numbers of clinical trials are evaluating therapeutic cancer vaccines that either target specific tumor-associated antigens, such as the CT antigens NY-ESO-1 or MAGEA3, or aim to transiently inhibit critical immune check points such as those mediating peripheral tolerance.<sup>3</sup> However, in many cases, the chronic nature of the disease makes it difficult to gain an early assessment of whether an individual patient is generating a therapeutically useful response following vaccination.

The expression of different CT antigens is known to be associated with many different types of cancer,<sup>4</sup> but the absence or presence of expression of any one CT antigen is not in itself exclusively indicative of any specific cancer.<sup>1</sup> It remains plausible though that patterns of CT antigen expression may prove useful as diagnostic markers of specific cancer types or as correlates of disease progression and response to therapy. However, to be viable as cancer biomarkers, CT antigen expression signatures should preferably be quantifiable in peripheral fluids to avoid unnecessarily invasive treatments and should be highly accurate for diagnostic and/or prognostic purposes to allow improved clinical management of patients.<sup>5–7</sup> One way in which this may be achieved is through the quantitative measurement of correlated anti-CT antigen autoantibody signatures in serum.

Protein microarray technology enables the high throughput, parallel analysis of a number of different molecular interactions under uniform assay conditions,<sup>8–15</sup> albeit not typically yielding robustly quantitative data, and in principle therefore enables identification of novel disease-specific serological markers that are not readily accessible by other proteomic technologies.<sup>16–18</sup>

Herein, we describe the development of a novel CT antigen microarray-based approach to quantify anti-CT antigen serum antibody responses in cancer patients. We illustrated the potential of our platform by profiling the anti-CT antigen autoimmune responses of a small cohort of melanoma patients before and post-treatment with a NY-ESO-1-based therapeutic vaccine currently undergoing clinical trials<sup>19,20</sup> and by cross-referencing these data to those obtained using a conventional ELISA-based approach.

**Material and Methods****Cloning of cancer-testis antigen genes**

A parental insect cell expression vector was constructed essentially according to previously published methods<sup>21</sup> (see

Supporting Information, Section S1 for details). In total, 100 full length proteins were cloned and expressed in insect cells as N-terminal fusions to the *Escherichia coli* BCCP protein domain<sup>22,23</sup> for printing on the CT100 array. Of these, 72 were CT antigen proteins, while the remaining 28 were other cancer-associated proteins/proteins of interest (see Table 1).

**Expression of CT antigens**

Recombinant CT antigens were expressed in insect cells using a previously published protocol.<sup>21</sup> The soluble, crude protein extracts were collected, the protein concentrations were determined by Bradford assay<sup>24</sup> and the extracts were stored at  $-80^{\circ}\text{C}$  before array printing. Expression of each antigen was assessed by western blot using a mouse anti-c-Myc antibody (1:5,000 dilution; Sigma-Aldrich, St. Louis, MO) followed by a goat anti-mouse IgG horseradish peroxidase (HRP) conjugate (1:25,000 dilution; KPL, Gaithersburg, MD). Biotinylation of each antigen was assessed by western blot using a streptavidin-HRP conjugate probe (1:40,000 dilution; GE Healthcare, Pittsburgh, PA).

**CT antigen microarray fabrication**

Crude lysates of each antigen were diluted 1:1 with PBS containing 40% sucrose. A total of 40  $\mu\text{L}$  of the diluted crude protein extract for each BCCP-tagged protein was transferred to individual wells of a 384-well V-bottom plate. The plate was centrifuged at 1,000g for 2 min at  $4^{\circ}\text{C}$  to pellet any residual cell debris and then kept at  $4^{\circ}\text{C}$  before and during the microarray print run.

Each CT100 array was printed on a streptavidin-coated microarray slide using a QArray2 robotic arrayer (Genetix, Berkshire, UK) equipped with  $8 \times 300 \mu\text{m}$  flat-tipped solid pins. In-house streptavidin-coated array surfaces were prepared essentially according to a previously published method<sup>25</sup> (see Supporting Information, Section S2 for details). Each array consisted of eight sub-arrays, with each sub-array printed by a different pin. The printing procedures were performed at room temperature (RT), while the source plate was kept at  $4^{\circ}\text{C}$  and the print chamber humidity was maintained at  $\sim 50\%$ . The arrays were printed using the following settings: inking time = 500 ms, microarraying pattern =  $7 \times 7$ , 642  $\mu\text{m}$  spacing, maximum stamps per ink = 1, number of stamps per spot = 2, printing depth =

**Table 1.** List of proteins on the CT100 cancer testis antigen array

|                |                |                     |                  |
|----------------|----------------|---------------------|------------------|
| BAGE5 (29%)    | SYCP1          | THEG                | <i>FES</i>       |
| CTAG2 (61%)    | NXF2           | TPTE                | <i>FGFR2</i>     |
| DDX53 (9%)     | NY-ESO-1 (61%) | TSGA10              | <i>MAPK1</i>     |
| GAGE1 (9%)     | NY-CO-45       | TSSK6               | <i>MAPK3</i>     |
| GAGE5 (11%)    | OIP5           | TTR                 | <i>p53</i>       |
| MAGEA1 (5%)    | PBK            | XAGE2               | <i>p53 S6A</i>   |
| MAGEA3 (8%)    | RELT (10%)     | XAGE3a v1           | <i>p53 S15A</i>  |
| MAGEA4 v2      | ROPN1          | XAGE3a v2           | <i>p53 T18A</i>  |
| MAGEA4 v3 (6%) | SGY-1          | ZNF165              | <i>p53 S46A</i>  |
| MAGEA4 v4      | SILV           | <i>AKT1</i>         | <i>p53 M133T</i> |
| MAGEA5         | SPAG9          | <i>CALM1</i>        | <i>p53 Q136X</i> |
| MAGEA10        | SPANXA1        | <i>CDC25A</i>       | <i>p53 C141Y</i> |
| MAGEA11        | SPANXB1        | <i>CDK2</i>         | <i>p53 L344P</i> |
| MAGEB1 (6%)    | SPANXC         | <i>CDK4</i>         | <i>p53 K382R</i> |
| MAGEB5         | SPANXD         | <i>CDK7</i>         | <i>p53 S392A</i> |
| MAGEB6         | SPO11          | <i>CPR (27%)</i>    | <i>PRK CZ</i>    |
| MART-1/MLANA   | SSX1           | <i>CREB1</i>        | <i>RAF</i>       |
| MICA           | SSX2a          | <i>CTNNB1</i>       | <i>SRC</i>       |
| MMA1           | SSX4           | <i>CYP3A4 (28%)</i> |                  |
| NLRP4          | SYCE1          | <i>EGFR</i>         |                  |

Note: Proteins in italics denote non-cancer testis antigens. (n%) refers to percentage of sera samples exhibiting a significant response (i.e., response observed in  $\geq 5\%$  of the patient sera samples in this study).

150  $\mu\text{m}$ , water washes = 60 sec wash and 0 sec dry, ethanol wash = 10 sec wash and 1 sec dry.

Replica CT100 arrays were printed in a four-plex format (i.e., four replica arrays per slide) using crude cell lysates. Each of the 100 cancer antigens was printed in triplicate within each array. The positive control consisted of biotinylated human IgG (50 ng/ $\mu\text{L}$ ; Rockland Immunochemicals, Gilbertsville, PA). The negative controls comprised biotinylated sheep IgG (200 ng/ $\mu\text{L}$ ; Rockland Immunochemicals) and a BCCP-tag only “empty vector” lysate control. In addition, three concentrations of biotinylated Cy5-biotin-BSA (5, 10 and 15 ng/ $\mu\text{L}$ ) were included in each sub-array for slide orientation and signal normalization purposes. The array design is shown in Supporting Information Figure S1.

After printing, each slide was washed for 30 min with 50 mL pre-chilled blocking solution (25 mM HEPES pH 7.5, 20% glycerol, 50 mM KCl, 0.1% Triton X-100, 0.1% BSA, 1 mM DTT and 50  $\mu\text{M}$  biotin) and stored at  $-20^\circ\text{C}$  submerged in storage buffer (25 mM HEPES pH 7.5, 50% glycerol, 50 mM KCl, 0.1% Triton X-100, 0.1% BSA and 1 mM DTT) until use.

#### Verification of immobilization of BCCP-tagged proteins to array surface

Mouse anti-c-Myc antibody was diluted 1:1,000 in 1 mL PBST containing 5% fat-free milk powder. One CT array

slide per batch was removed from the storage buffer, equilibrated in PBST at RT for 5 min, the PBST removed and the array incubated with 5 mL antibody solution with gentle agitation at RT for 30 min. The array was washed for  $3 \times 5$  min with 1 mL PBST and incubated with goat anti-mouse antibody-HRP conjugate (1:1,000 dilution in 1 mL milk/PBST) with gentle agitation at RT for 30 min. The array was washed for  $3 \times 5$  min with 1 mL PBST, submerged in 5 mL chemiluminescent detection reagents (Thermo Scientific) for 1 min, dried by centrifugation and detected using autoradiography.

#### Linearity and dynamic range microarray assays

To determine the optimal serum and anti-human IgG antibody dilutions for the detection of antigen binding, replica arrays were printed in a 16-plex format using a single NY-ESO-1 crude lysate at various dilutions (see below). This antigen was printed in two sets of triplicates within each array, along with a loading control (16 ng/ $\mu\text{L}$  biotinylated Cy5-BSA) and a “lysis buffer only” negative control. Each array was printed and blocked as above, except that a single 300  $\mu\text{m}$  flat-tipped solid pin was used; each slide was assayed on the day of printing.

An initial linearity assay was performed in duplicate using serial dilutions of a single serum sample (P117, day 483) at 1:50, 1:100, 1:200, 1:400, 1:800, 1:1,600, 1:3,200 and 1:6,400 dilutions in PBST. A 16-chamber silicone gasket (Flexwell incubation chamber; Grace Bio-Labs, OR) and a 16-chamber metal gasket (ProPlate slide chamber system; Grace Bio-Labs), were assembled over a freshly printed, blocked and washed slide. A serum volume of 45  $\mu\text{L}$  was added to each gasket chamber, incubated at RT for 1 hr, and each chamber was then washed independently with PBST. Cy3-labeled goat anti-human IgG (45  $\mu\text{L}$  diluted in PBST to 20  $\mu\text{g}/\text{mL}$ ; Invitrogen, Carlsbad, CA) was added to each chamber and incubated for 1 hr at RT. The gasket was removed and the slide was washed in PBST, dried and scanned at various gain settings on an LS Reloaded fluorescence microarray scanner (Tecan Group, Männedorf, Switzerland).

A further linearity assay was performed using serum dilutions 1:200 and 1:2,400 (P117, day 483) in a 16-plex format, with each serum dilution (45  $\mu\text{L}$ ) added to a separate individual array. After incubation as above, each array was washed independently and Cy3-labeled goat anti-human IgG (45  $\mu\text{L}$  diluted in PBST to final concentrations of 1.25, 2.5, 5, 10, 15, 20, 30 and 40  $\mu\text{g}/\text{mL}$ ) was then incubated on duplicate individual arrays for 1 hr at RT. The slide was washed in PBST, dried and scanned.

A dynamic range assay was similarly performed in duplicate using serial dilutions (1:1,000, 1:2,000, 1:4,000, 1:8,000, 1:16,000, 1:32,000, 1:64,000 and 1:128,000) of the same serum sample and Cy3-labeled goat anti-human IgG (20  $\mu\text{g}/\text{mL}$ ).

#### Quantification of the absolute array detection limit for CT antigens

To estimate the absolute detection limit of our CT antigen microarray platform, three further assays were performed

using the same serum sample as for the linearity assays. Absolute total protein concentration was determined by Bradford assay; SDS-PAGE-based densitometry analysis (Gene Tools; Syngene, Cambridge, UK) was used to determine the proportion of total protein corresponding to total IgG; and a protein microarray assay was performed to determine the proportion of total IgG corresponding to anti-NY-ESO-1. This last assay was performed in quadruplicate as follows: replica 16-plex arrays of the serum sample (1:800 dilution in 1 M PPB pH 8.0, supplemented with 15% glycerol (v/v)), were printed on an un-derivatised Nexterion H slide using a single 300  $\mu\text{m}$  flat-tipped solid pin, unreacted NHS esters were blocked (1 hr in chilled 50 mM PPB, supplemented with 50 mM ethanolamine), and 45  $\mu\text{L}$  anti-human IgG (100 ng/ $\mu\text{L}$ ), NY-ESO-1-BCCP crude insect cell lysate (1:20 dilution), insect cell lysate (1:20 dilution), or buffer only control were incubated on discrete replica arrays (1 hr at RT). Each array was washed independently with PPB, and Cy5-labelled streptavidin (1  $\mu\text{g}/\text{mL}$  in PBST; GE Healthcare) was incubated on each replica array for 1 hr at RT, after which the slide was washed, dried and scanned as before.

#### Microarray data extraction

All raw image files were visually inspected to assess spot morphology and background signal. Any arrays showing high background, excessive speckling, the presence of interfering dust particles or fibers, or evidence of coalescing protein spots were re-run. Typically, <10% of assays were repeated for these reasons. In ArrayPro Analyzer software (Media Cybernetics, Rockville, MD), a grid was autoaligned over the individual spots on each scanned image file and a constant area feature finder was used across the array surface. Following automatic spot finding, manual curation of the grid alignment was performed. A "GAL" file containing information on the sample identity in each spot was read into ArrayPro and the raw data was extracted from each spot as well as the local background in batch processing mode using a 200 RFU pixel threshold, yielding the median foreground and background pixel intensities per sample spot.

#### Assay of the CT100 arrays with patient sera

A total of 140 serum samples from 46 stage III and IV malignant melanoma patients were provided by the Ludwig Institute for Cancer Research (LICR; Melbourne, Australia) from an NY-ESO-1 ISCOMATRIX® CT antigen-based vaccine Phase II clinical trial, LUD2002-013.<sup>20</sup> Informed consent was obtained and our study was conducted after review by the Human Research Ethics Committees (LICR HREC2003/01660, UCT HREC 240/2011).

Serum samples were taken at time points before receiving vaccination (Day 0) and then two weeks after further vaccination boosters, *e.g.*, at days 70 and 154 (note that not all patients had the same number of vaccination boosters nor were these all performed at the same intervals). Control sera were provided by 14 healthy volunteers.

Individual arrays were each incubated with a unique serum sample (60  $\mu\text{L}$  at 1:200 dilution) for 1 hr at RT, washed, and incubated with 60  $\mu\text{L}$  Cy5-labeled goat anti-human IgG (Invitrogen; 1:100 dilution in PBST) for 1 hr at RT. The individual arrays were then washed, dried and scanned at fixed gain settings of 110, 120, 125 and 135 PMT. All liquid handling steps were performed on a HS4800 Pro automated hybridization station (Tecan Group).

For stability trials, replica arrays from a single print batch were similarly assayed in quadruplicate over a four week period, using the same serum sample each time. Eight further arrays were used to investigate the effect of increased temperature (RT vs. 37°C) on assay performance.

#### CT100 array data processing and analysis

Our group has previously developed a bioinformatic pipeline for pre-processing and quality control of custom protein microarray data,<sup>26</sup> (see Supporting Information, Section S3 for details), which we have automated in a Java script.

Sub-arrays within each array were normalized with respect to each other to minimize any effects of pin-to-pin variation. Whole arrays were then normalized with respect to each other to minimize any effects of slide-to-slide variation. Both normalization steps were performed using 5 ng/ $\mu\text{L}$  Cy5-biotin-BSA as the control. A novel composite normalization method combining both quantile and total intensity normalization modules was used for these purposes, as described previously.<sup>26</sup> Any assays with unsatisfactory CV values were repeated.

## Results

### Cloning and expression of CT antigens as BCCP-fusion proteins

Recombinant gene cloning methods were used to insert a total of 72 CT antigen and 28 non-CT antigen genes into a baculoviral expression vector as N-terminal fusions to an *E. coli*-derived biotin-carboxyl carrier protein (BCCP) tag carrying a c-Myc tag (see Table 1 for the full list of antigens). The BCCP-tag is biotinylated *in vivo*, enabling single-step immobilization and purification of folded, BCCP-tagged recombinant proteins by printing crude lysates directly onto streptavidin-coated, PEG-derivatised microarray surfaces under native conditions; the very high affinity ( $K_d \sim 10^{-15}$  M)<sup>9</sup> and specificity of the streptavidin-biotin interaction combined with the intrinsic resistance of PEG surfaces to non-specific protein adsorption<sup>27</sup> enabled avoidance of laborious pre-purification of each recombinant protein under denaturing conditions.<sup>18</sup>

In the absence of any pre-purification step, it might be expected that host cell proteins that are endogenously biotinylated and observed in western blots would compete with the biotinylated recombinant proteins for available streptavidin-binding sites on the array surface. However, under native conditions we have observed that these endogenous biotinylated proteins do not compete efficiently with biotinylated recombinant proteins for binding,<sup>28</sup> probably because in such endogenous proteins

the biotin moiety is typically buried<sup>29</sup> and therefore not physically available to bind streptavidin under native conditions.

This recombinant insect cell expression approach gave a >95% success rate from cloned, sequence-verified transfer vector to expressed, folded and biotinylated proteins suitable for array fabrication; this compares favorably with the lower success rates observed when attempting to express mammalian proteins in *E. coli*.<sup>30</sup> Western blotting was used to confirm biotinylation of the expressed recombinant proteins, and the addition of free biotin to the growth medium was observed to increase the extent of biotinylation of the recombinant BCCP fusion proteins (data not shown) despite the absence of a co-expressed *E. coli* biotin ligase.

All recombinant proteins were expressed under the same conditions, with no attempt made to maximize expression levels. We estimated there to be a limiting number of available biotin-binding sites on the streptavidin-coated microarray surface, and the high affinity of the streptavidin-biotin interaction means that the surfaces saturate with antigen even at low antigen expression levels. This provides a crude normalization of protein loading without the need to pre-adjust the concentrations of the individual crude lysates to compensate for differences in expression levels before array fabrication.<sup>9</sup>

### CT antigen microarray fabrication

In a single print run, 68 replica CT100 protein microarrays could be printed in a four-plex format (Supporting Information Fig. S1), with each spotting event delivering ~10 nL sample; glycerol and sucrose were included in the printing buffer to reduce evaporation rates and to control spot sizes. Due to the very small volumes required, each 50 µL aliquot of harvested expression cells provided enough recombinant protein to print 25 replica slides in four-plex format, with each protein printed in triplicate in each array. Therefore, one 3 mL baculovirus culture yielded sufficient expressed protein to fabricate 700 replica arrays, or >2,000 replica spots of each protein, thereby aiding reproducibility.

Using  $8 \times 300 \mu\text{m}$  solid pins, each array was printed in eight blocks of  $7 \times 7$  spots (*i.e.*, 392 discrete protein spots per array) with a spot-to-spot spacing of 642 µm. In principle, this format enables up to 130 individual protein types to be printed in triplicate in each of the four array fields per slide.

### Microarray linearity, dynamic range and limits of detection

Robust linearity and dynamic range experiments were performed to determine the optimal serum and anti-human IgG antibody dilutions for the detection of antigen binding. All data generated by the protein arrays for these assays were pre-processed and analyzed as described in Materials and Methods. No data points were excluded by the data filtering steps, indicating that the arrays were of good quality.

From the initial linearity assay, a classic saturation binding curve (Fig. 1a) indicated that at serum dilutions of ~1:50 of a randomly chosen serum sample demonstrating a high

response to NY-ESO-1 (P117, day 483), the available NY-ESO-1 binding sites on the microarray were saturated ( $B_{\text{max}} = 55,370$  RFU), with half-maximal binding occurring at ~1:1,250 dilution. This corresponds with the known high immunogenicity of NY-ESO-1.<sup>31</sup>

To exclude the possibility that the observed saturation binding occurred due to limiting secondary antibody availability, an assay was performed using two different serum dilutions (1:200 and 1:2,400) and a range of secondary antibody concentrations. At both serum dilutions, saturation of secondary antibody binding was reached at ~10 µg/mL ( $B_{\text{max}} = 58,936$  RFU; Fig. 1b), with a calculated binding affinity ( $K_d$ ) of the primary–secondary antibody interaction on the array surface of ~2 µg/mL. This confirmed that the data in Figure 1a reflected the saturation binding of the serum auto-antibodies to the immobilized antigens, rather than a limiting quantity of secondary antibody; 20 µg/mL secondary antibody were therefore used in all further assays.

A dynamic range assay revealed a linear response over greater than three orders of magnitude (Fig. 1c) and no evidence of signal limitation was observed at the serum dilutions tested; even at the highest tested dilution (1:128,000), a measurable signal was still detectable well above the median background values (Supporting Information Table S1). By extrapolation of the linear range to the lower limit and assuming a noise threshold of two standard deviations (SD) of the background, the detection limit was estimated to be ~1:1,000,000 serum dilution, corresponding to an autoantibody titer of ~190 pg/mL.

### Quality control of the fabricated CT100 arrays

Before use, each batch of printed arrays was quality tested using an anti-c-Myc assay to confirm immobilization of the BCCP-tagged proteins. Using an automated hybridization system, each array on each four-plex slide could be assayed under independent conditions and 24 arrays could be assayed per run. Increasing the temperature at which antibody binding assays were performed to 37°C had no significant effect on the anti-c-Myc assays but decreased serum antibody binding was observed so room temperature was used for all further assays. Stability studies on the CT100 arrays showed no loss of assay performance over a three week period post-printing, but thereafter a marked decline in signal intensity for replica arrays was observed (data not shown), possibly due to a slow, time-dependent burial of the arrayed antigens through the polyethylene glycol coating on the surface. All slides in our study were therefore used within 3 weeks of printing.

### Using the CT100 array to analyze serum-based immune response to various CT antigens

Serum samples were obtained from 46 patients before vaccination with a NY-ESO-1-based vaccination (Day 0) and then 2 weeks after further repeated vaccination boosters (*e.g.*, at Days 70 and 154). A total of 140 patient serum samples plus

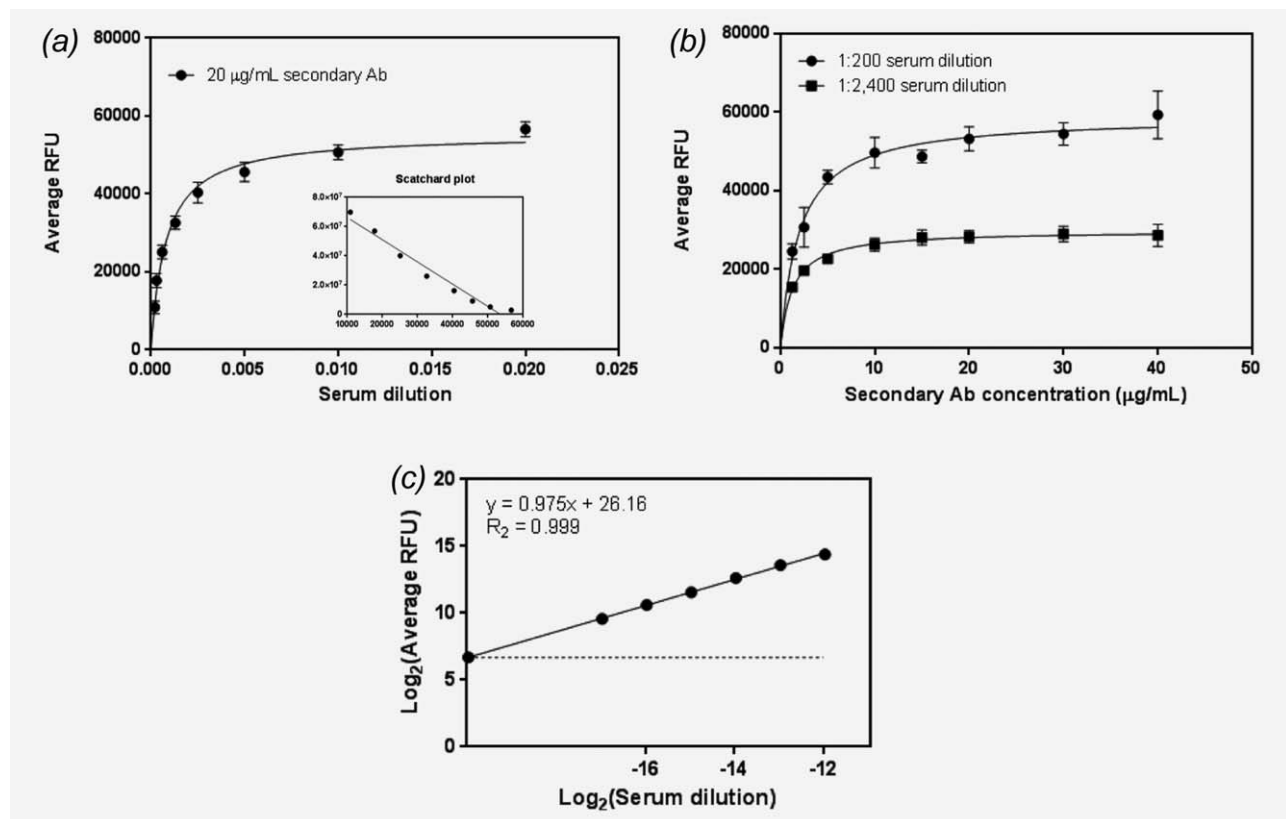


**Figure 1.** Linearity and dynamic range assays of autoantibody detection on the array surface. (a) Initial linearity assay using a series of serum dilutions of a randomly chosen patient sample (P117, Day 483) to measure saturation binding of patient autoantibodies to the NY-ESO-1 antigen on the array surface, using 20 µg/mL secondary Ab for detection. Inset: Scatchard plot of the same data. (b) A second linearity assay using two serum dilutions (1:200 and 1:2,400) of the same patient sample and a range of secondary Ab concentrations to determine the dynamic range of secondary Ab binding. (c) A dynamic range assay indicating the linear range of the platform. The limit of detection (~1:1,000,000 serum dilution) is where the data intersects with the signal cut-off level (two standard deviations of the background; indicated here as the dashed line).

sera from 14 healthy volunteers were analyzed individually on replica CT100 arrays; all array images were manually inspected for obvious defects, after which pin-to-pin normalization and rigorous data filtering was performed using an automated Java script developed by our group.<sup>26</sup> An autoantibody response was observed for most patients at the first time point available for each (note that here we refer to an autoantibody response to treatment without implying any clinical endpoint, such as possible correlations to tumor regression or patient improvement), and Figure 2 shows the relative change in serological titers over time for a representative subset of patients.

Of the 100 CT antigens/non-cancer antigens on the CT100 microarray, 13 antigens showed autoantibody binding signals significantly greater than that of the negative controls in >5% of the patient sera samples (Table 1). As expected, the NY-ESO-1 vaccine antigen exhibited the greatest overall autoantibody response (~61% of patients) whilst assays using sera from 14 presumed healthy volunteers showed no significant binding to any arrayed antigen (data not shown). Autoantibody responses to CTAG2 (otherwise known as LAGE-1/

NY-ESO-2) were observed in a similar number of patients to NY-ESO-1, most likely due to the high homology (84%) between these two proteins<sup>32</sup> resulting in antibody recognition of shared epitopes. However, the ratio of NY-ESO-1 to CTAG2 autoantibody titres was found to vary considerably across individual patients, suggesting that different patients raised autoantibodies to different epitopes along the length of the NY-ESO-1 protein (Fig. 3), in agreement with previous observations.<sup>33</sup>

Only a small proportion (13%) of patients showed no appreciable autoantibody response to the vaccine, possibly due to the immune-suppressive effects of prolonged medical treatments. In contrast, a high anti-NY-ESO-1 autoantibody titer was observed for 38% of patients before vaccination, probably due to spontaneous recognition of endogenous tumor antigen, since these patients all presented with advanced metastatic melanoma.

The protein array data generated here was compared to ELISA data generated independently by LICR for a subset of 22 patients (Supporting Information Table S2); 18 patients identified as responders by ELISA were also observed to be

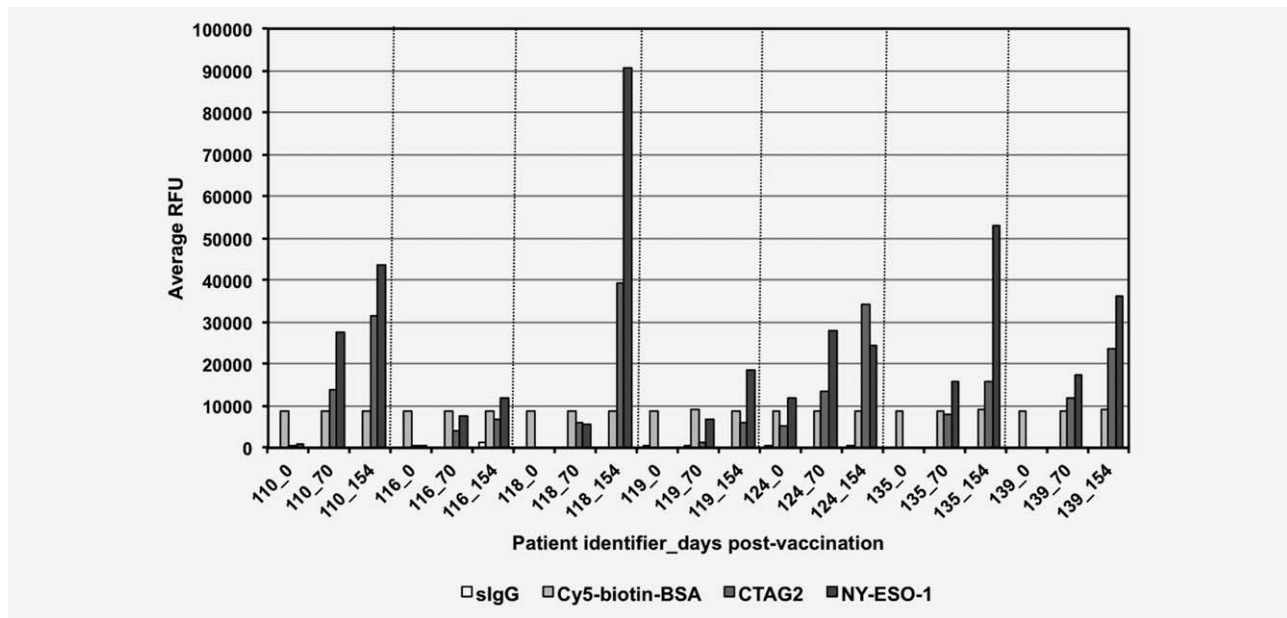


**Figure 2.** Representative data from a subset of patients. Patients with serum samples at time points 0, 70 and 154 days post-vaccination are illustrated here, demonstrating the increase over time of autoantibody response to the CTAG2 and NY-ESO-1 antigens. A negative control (slgG) and loading control (Cy5-biotin-BSA) are included for comparison.

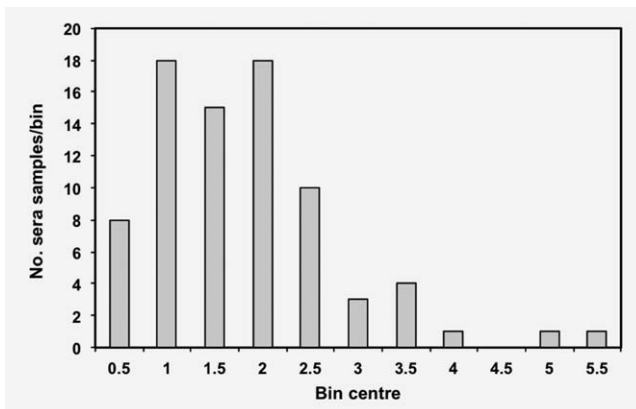


**Figure 3.** Patient variability in NY-ESO-1 epitope recognition sites. Histogram depicting the distribution of patient sera samples exhibiting a specified ratio of NY-ESO-1/CTAG2 immune response. The antigen CTAG2 exhibits high homology to NY-ESO-1, and the varying NY-ESO-1/CTAG2 ratios suggests that patients raise autoantibodies to different NY-ESO-1 epitopes along the length of the antigen.

responders by protein array data. A further three responders were detected only by the protein microarray method; the likelihood that these represent false positives is reduced by the corresponding observation of significant anti-CTAG2 binding on the microarrays for these patients. The patients determined by ELISA to have high initial Ab titer on Day 0 also all had high signals on our arrays, with an additional high initial titer patient detected by the microarray assays. These data suggest that our cancer antigen microarray platform is at least as sensitive as ELISA (currently the gold

standard for measuring Ab-antigen interactions) whilst more highly multiplexed.

In addition to the NY-ESO-1 and CTAG2 antigens, several other CT antigens were observed to elicit immune responses in individual patients, including members of the BAGE, GAGE and MAGE groups, which are all known to be associated with melanoma.<sup>32,34–36</sup> Interestingly, in patient samples exhibiting an autoantibody response to the 13 most commonly observed antigens, with the exception of NY-ESO-1 and CTAG2 these responses appear reasonably consistent between different time points for a given patient, as perhaps expected, but appear randomly distributed between different patients (Fig. 4); these distinguishable patterns of autoantibody responses between patients may later provide correlates to treatment response and disease progression and are therefore an important avenue for further research using larger patient cohorts.

CTAG2 and NY-ESO-1 both showed significant changes in autoantibody response over the various time points measured (Supporting Information Fig. S2), confirming that the majority of patients responded to the initial and booster vaccinations. However, the increase in autoantibody titer for NY-ESO-1 did not significantly correlate in our cohort with a change in autoantibody response to any of the other CT antigens represented on this first generation CT antigen microarray, nor did it correlate with therapeutic response (data not shown). Notably, a subset of 18 patients showed strong anti-NY-ESO-1 responses post-vaccination, despite not displaying any anti-NY-ESO-1 antibody titer pre-vaccination.

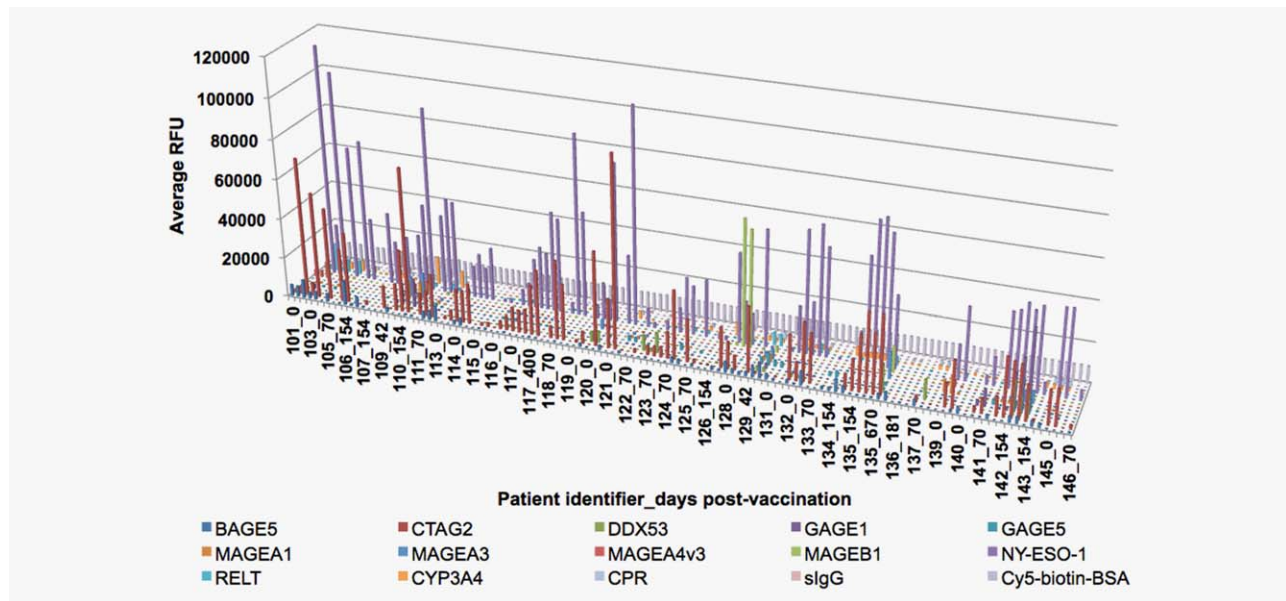


**Figure 4.** Graph across patient sera samples depicting the clustering of immune response to various antigens of interest. Patient samples exhibiting an immune response to one or more of the 13 antigens of interest also demonstrated clustering of antigen responses across the same individual patients. A negative control (slgG) and loading control (Cy5-biotin-BSA) are included for comparison.

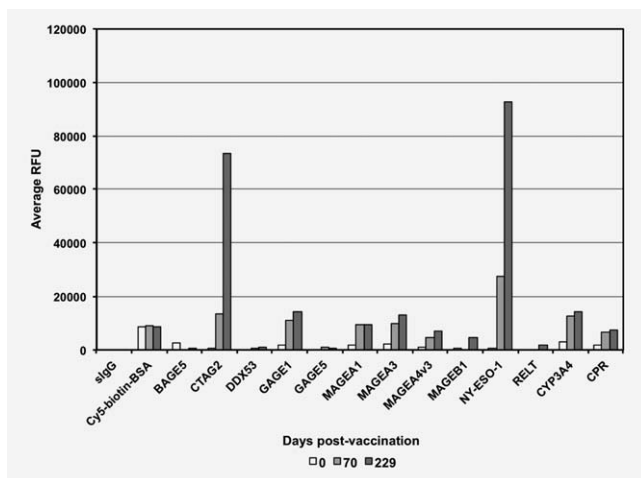


**Figure 5.** Preliminary evidence of determinant spreading. A number of patients exhibited evidence of determinant spreading across several antigens of interest over various points post-vaccination. Patient 110 is shown here as a representative example.

Evidence of “determinant spreading” (used here as the induction of an autoantibody response to multiple antigens subsequent to an initial autoantibody response to the vaccine target)<sup>37</sup> was also observed amongst some responders. One patient in particular, P110, showed strong autoantibody responses post-vaccination to five of the 13 antigens commonly observed to elicit autoantibody responses in our study (Fig. 5).

**Discussion**

The quantitative study of antibodies that recognize cancer antigens in patients could in principle enable, *inter alia*, early

detection of tumors, patient stratification, personalized patient treatment, development of improved therapies, and more efficient monitoring of therapeutic response and disease progression.

The cancer-testis antigen microarray approach described here has the advantage of providing data on cancer antigen expression through direct quantitation of autoantibody titers in serum rather than through the binding of human antigens to, for example, murine antibodies. Monoclonal antibodies raised by animal immunization approaches typically have target affinities in the nanomolar to sub-nanomolar range; in practice this means that these antibodies can only detect target antigens in serum at nanomolar concentrations or above, at which levels there are likely to already be sufficient symptoms for diagnosis based on a physical examination. By contrast, human autoantibodies are thought to be elicited relatively early in tumorigenesis<sup>38</sup> and bind to their target autoantigens with high affinities and specificities, thus making detection of cancer-specific autoantibodies possible in principle at significantly lower serum concentrations than is routinely possible for detection of the cancer antigens themselves, thereby leading to the potential for pre-symptomatic cancer diagnosis.

Herein, we have shown that oriented and folded CT anti-gen microarrays can detect and quantify the presence of large panels of specific human autoantibodies in serum with a detection limit in the pg/mL range, with linearity over at least three orders of magnitude and with low non-specific binding to the arrayed antigens in healthy controls, representing a significant advance in the field compared to ELISA or other protein microarray platforms. In addition, our use of insect cell-expressed recombinant antigens fused to the compact E.

*coli* BCCP protein domain, which is biotinylated *in vivo* in insect cells,<sup>22,23</sup> enables facile, single-step antigen microarray fabrication without laborious pre-purification of the target antigens. Furthermore, the potential for non-specific binding to obfuscate biologically meaningful serological data (as occurs in many other protein microarray platforms) is averted by our use of folded antigen arrays in combination with PEG-coated microarray surfaces, which together minimize unwanted binding of immunoglobulins to unfolded, exposed hydrophobic regions of arrayed proteins or to the underlying array surface; this therefore represents an additional advantage of our platform over other antigen microarray systems. Overall, our CT antigen microarray platform thus represents a robust, sensitive, high-throughput and readily customizable means to quantify specific autoimmune profiles in patient sera.

Using this platform, we have demonstrated apparently increased sensitivity compared to ELISA for measuring antibody responses to vaccination, whilst at the same time allowing the simultaneous and rapid determination of autoantibody titers against almost a hundred other cancer antigens in the same sample. As with ELISAs, in our work we have not adjusted serum dilutions to account for variations in total IgG concentration between samples, but inclusion of an anti-human-IgG antibody on our microarray would enable this to be factored in post-assay if needed.

We have applied our platform to the investigation of autoantibody profiles in a small cohort of melanoma patient sera and observed a number of discrete patient autoimmune profile types. Simplistically, patients could be classified distinctly as “autoantibody responders” (87% of the cohort, comprising both those with and without an initial high titer of anti-NY-ESO-1 antibody), or as “autoantibody non-responders.” However, it remains to be seen whether the pre-existence or induction of an anti-NY-ESO-1 titer correlates with later clinical improvements post-vaccination amongst these patients, or whether other, more subtle, quantitative immunological features that can only be revealed *via* a multiplexed antigen microarray, such as that described here, will provide correlates of therapeutic response. It is interesting in this regard that our CT antigen array data provides preliminary evidence of determinant spreading to other antigens in individual patients post-vaccination, as well as direct evidence of varied NY-ESO-1 epitope recognition between patients. Both of these phenomena were previously unrecognized in this cohort and might conceivably impact on clinical outcome;

further studies are now underway to explore the clinical relevance of these observations in a larger cohort.

It is notable that the NY-ESO-1 vaccine used in the underlying clinical trial was designed to elicit a T-cell response,<sup>19,33</sup> yet here we have profiled B-cell responses to NY-ESO-1 and other CT antigens and it remains to be seen how well the autoantibody profiles correlate with T-cell responses in these same patients. However, given that T-cell and B-cell responses are coordinated to some degree at the level of T-helper cells, the observation of significant, pre-existing patient-specific autoantibody titers to NY-ESO-1 at minimum serves to confirm both the aberrant expression of the intended vaccine target as well as its recognition as an autoantigen in those patients.

In this melanoma cohort, we have identified previously unknown, patient-specific autoantibody responses to numerous CT antigens in addition to the intended vaccine target, suggesting that further exploration of these antigens as potential biomarkers of vaccine response or of cancer prognosis is warranted. Furthermore, our platform may now provide a practical route to patient stratification before therapeutic vaccination: for example, patients who present with melanomas but without a measurable, pre-existing anti-NY-ESO-1 autoantibody titer may either not express NY-ESO-1 in the tumor, or may recognize it as a self-antigen; in either case, anti-NY-ESO-1 vaccine efficacy is likely to be affected, yet the same patients may respond to a different vaccine, depending on their cancer antigen expression profiles, which can now be easily determined pre-vaccination using our cancer antigen microarray approach. We therefore anticipate that our novel, quantitative, customizable CT antigen microarray platform will find considerable usage in future cancer research, both in patient stratification as well as in monitoring patient responses to treatment.

### Acknowledgements

J.M.B. thanks the Department of Science & Technology and the National Research Foundation for a South African Research Chair Initiative grant. T.J. was the recipient of a Victorian Cancer Agency Fellowship. J.D. was the recipient of bursaries from the University of Cape Town and the Marion Beatrice Waddel Foundation. We thank the Centre for Proteomic & Genomic Research, Cape Town, for access to protein microarray equipment.

### References

1. Scanlan MJ, Gure AO, Old LJ, et al. Cancer/testis antigens: an expanding family of targets for cancer immunotherapy. *Immunol Rev* 2002;188: 22–32.
2. Hunder NN, Wallen H, Cao J, et al. Treatment of metastatic melanoma with autologous CD4+ T cells against NY-ESO-1. *N Engl J Med* 2008; 358:2698–703.
3. Ueda H, Howson JMM, Esposito L, et al. Association of the T-cell regulatory gene CTLA4 with susceptibility to autoimmune disease. *Nature* 2003;423:506–11.
4. Simpson AJG, Caballero OL, Jungbluth A, et al. Cancer/testis antigens, gametogenesis and cancer. *Nat Rev Cancer* 2005;5:615–26.
5. Berrade L, Garcia AE, Camarero JA. Protein microarrays: novel developments and applications. *Pharm Res* 2011;28:1480–99.
6. Frank R, Hargreaves R. Clinical biomarkers in drug discovery and development. *Nat Rev* 2003;2: 566–80.
7. Rifai N, Gillette MA, Carr SA. Protein biomarker discovery and validation: the long and uncertain

- path to clinical utility. *Nat Biotechnol* 2006;24:971–83.
8. Wolf-Yadlin A, Sevecka M, MacBeath G. Dissecting protein function and signaling using protein microarrays. *Curr Opin Chem Biol* 2009;13:398–405.
  9. Boutell JM, Hart DJ, Godber BLJ, et al. Analysis of the effect of clinically-relevant mutations on p53 function using protein microarray technology. *Proteomics* 2004;4:1950–8.
  10. Kodadek T. Protein microarrays: prospects and problems. *Chem Biol* 2001;8:105–15.
  11. Predki PF. Functional protein microarrays: ripe for discovery. *Curr Opin Chem Biol* 2004;8:8–13.
  12. Zhu H, Klemic JF, Chang S, et al. Analysis of yeast protein kinases using protein chips. *Nat Genet* 2000;26:283–9.
  13. Zhu H, Bilgin M, Bangham R, et al. Global analysis of protein activities using proteome chips. *Science* 2001;293:2101–5.
  14. Michaud G, Salcius M, Zhou F, et al. Analyzing antibody specificity with whole proteome microarrays. *Nat Biotechnol* 2003;21:1509–12.
  15. Fang Y, Lahiri J, Picard L. G protein-coupled receptor microarrays for drug discovery. *Drug Discov Today* 2003;8:755–61.
  16. Matarraz S, María MG, Alberto J, et al. New technologies in cancer. Protein microarrays for biomarker discovery. *Clin Transl Oncol* 2011;13:156–61.
  17. Sanchez-Carbayo M. Antibody microarrays as tools for biomarker discovery. In: Korf U, ed. *Methods in molecular biology*, vol. 785. New York: Humana Press Inc., 2011. 159–82.
  18. O’Kane SL, O’Brien JK, Cahill DJ. Optimized autoantibody profiling on protein arrays. In: Korf U, ed. *Methods in molecular biology*, vol. 785. New York: Humana Press Inc., 2011. 331–41.
  19. Davis ID, Chen W, Jackson H, et al. Recombinant NY-ESO-1 protein with ISCOMATRIX adjuvant induces broad integrated antibody and Cd4+ and Cd8+ T cell responses in humans. *Proc Natl Acad Sci USA* 2004;101:10697–702.
  20. Nicholaou T, Chen W, Davis ID, et al. Immunoe-diting and persistence of antigen-specific immunity in patients who have previously been vaccinated with NY-ESO-1 protein formulated in ISCOMATRIX. *Cancer Immunol Immunother* 2011;60:1625–37.
  21. Blackburn JM, Shoko A. Protein function microarrays for customised systems-oriented proteome analysis. In: Korf U, ed. *Methods in molecular biology*, vol. 785. New York: Humana Press Inc., 2011. 305–30.
  22. Athappilly FK, Hendrickson WA. Structure of the biotinyl domain of acetyl-coenzyme A carboxylase determined by MAD phasing. *Structure* 1995;3:1407–19.
  23. Chapman-Smith A, Cronan JE. The enzymatic biotinylation of proteins: a post-translational modification of exceptional specificity. *Trends Biochem Sci* 1999;24:359–63.
  24. Bradford MM. A rapid and sensitive method for the quantitation of microgram quantities of protein utilizing the principle of protein-dye binding. *Anal Biochem* 1976;72:248–54.
  25. Blackburn JM, Shoko A, Beeton-Kempen N. Miniaturized, microarray-based assays for chemical proteomic studies of protein function. In: Zanders E, ed. *Methods in molecular biology*, vol. 800. New York: Humana Press Inc., 2012. 133–162.
  26. Duarte J, Serufuri J-M, Mulder N, et al. Protein function microarrays: design, use and bioinformatic analysis in cancer biomarker discovery and quantitation. In: Wang X, ed. *Bioinformatics of human proteomics*. Springer, 2013. 39–74.
  27. Zheng J, Li L, Tsao H-K, et al. Strong repulsive forces between protein and oligo (ethylene glycol) self-assembled monolayers: a molecular simulation study. *Biophys J* 2005;89:158–66.
  28. Koopmann J-O, Blackburn J. High affinity capture surface for matrix-assisted laser desorption/ionisation compatible protein microarrays. *Rapid Commun Mass Spectrom* 2003;17:455–62.
  29. Choi-Rhee E, Cronan JE. The biotin carboxylase-biotin carboxyl carrier protein complex of *Escherichia coli* acetyl-CoA carboxylase. *J Biol Chem* 2003;278:30806–12.
  30. Terwilliger TC, Stuart D, Yokoyama S. Lessons from structural genomics. *Annu Rev Biophys* 2009;38:371–83.
  31. Nicholaou T, Ebert L, Davis ID, et al. Directions in the immune targeting of cancer: lessons learned from the cancer-testis Ag NY-ESO-1. *Immunol Cell Biol* 2006;84:303–17.
  32. Vaughan H, Svobodova S, Macgregor D, et al. Immunohistochemical and molecular analysis of human melanomas for expression of the human cancer-testis antigens NY-ESO-1 and LAGE-1. *Clin Cancer Res* 2004;10:396–404.
  33. Komatsu N, Jackson HM, Chan KF, et al. Fine-mapping naturally occurring NY-ESO-1 antibody epitopes in melanoma patients’ sera using short overlapping peptides and full-length recombinant protein. *Mol Immunol* 2013;54:465–71.
  34. Kirkin AF, Dzhandzhugazyan K, Zeuthen J. Melanoma-associated antigens recognized by cytotoxic T lymphocytes. *APMIS* 1998;106:665–79.
  35. Westbrook VA, Schoppee PD, Diekmann AB, et al. Genomic organization, incidence, and localization of the SPAN-X family of cancer-testis antigens in melanoma tumors and cell lines. *Clin Cancer Res* 2004;10:101–12.
  36. Svobodová S, Browning J, MacGregor D, et al. Cancer-testis antigen expression in primary cutaneous melanoma has independent prognostic value comparable to that of Breslow thickness, ulceration and mitotic rate. *Eur J Cancer* 2011;47:460–9.
  37. Butterfield LH, Ribas A, Disette VB, et al. Determinant spreading associated with clinical response in dendritic cell-based immunotherapy for malignant melanoma. *Clin Cancer Res* 2003;9:998–1008.
  38. Anderson KS, LaBaer J. The sentinel within: exploiting the immune system for cancer biomarkers. *J Proteome Res* 2005;4:1123–33.